

On the Role of Rotation Equivariance in Monocular 3D Human Pose Estimation

Pavlo Melnyk¹, Cuong Le¹, Urs Waldmann¹,
Per-Erik Forssén¹, and Bastian Wandt²

¹ Computer Vision Laboratory, Linköping University, Linköping 58331, Sweden

² Independent Researcher

pavlo.melnyk@liu.se

Abstract. Estimating 3D from 2D is one of the central tasks in computer vision. In this work, we consider the monocular setting, *i.e.* single-view input, for 3D human pose estimation (HPE). Here, the task is to predict a 3D point set of human skeletal joints from a single 2D input image. While by definition this is an ill-posed problem, recent work has presented methods that solve it with up to several-centimetre error. Typically, these methods employ a two-step approach, where the first step is to detect the 2D skeletal joints in the input image, followed by the step of 2D-to-3D lifting. We find that common lifting models fail when encountering a rotated input. We argue that learning a single human pose along with its in-plane rotations is considerably easier and more geometrically grounded than directly learning a point-to-point mapping. Furthermore, our intuition is that endowing the model with the notion of rotation equivariance without explicitly constraining its parameter space should lead to a more straightforward learning process than one with equivariance by design. Utilising the common HPE benchmarks, we confirm that the 2D rotation equivariance per se improves the model performance on human poses akin to rotations in the image plane, and can be efficiently and straightforwardly learned by augmentation, outperforming state-of-the-art equivariant-by-design methods.

Keywords: Equivariance · Human pose estimation · 2D-3D lifting

1 Introduction

Predicting 3D structures from 2D images is a fundamental task in computer vision. The problem, however, becomes ill-posed when the setting is constrained by single-view (*i.e.* monocular) estimation and unknown camera parameters. In this paper, we consider this setting within the task of monocular 3D human pose estimation (HPE), where the goal is to estimate 3D human skeletal joints from a single 2D image.

While there exist methods that solve this task in an end-to-end manner, a common approach is two-stage: 1) detect 2D keypoints from the input image, *e.g.* by using a pre-trained detector such as HRNet [4], and 2) lift the detected 2D

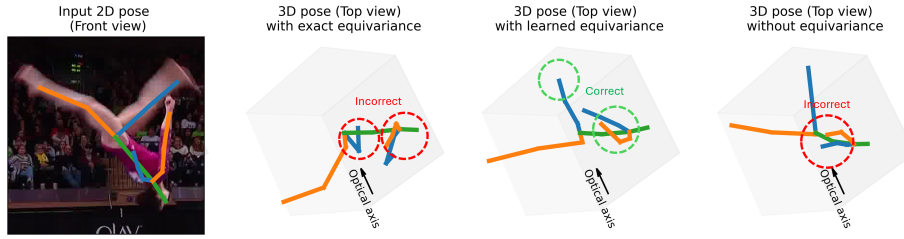


Fig. 1. Teaser: Learning rotation equivariance improves the performance of a 2D→3D lifting model in monocular human pose estimation for motions akin to rotations in the image plane. In contrast, typical lifting models lack this notion of equivariance. Furthermore, models that are equivariant by design over-constrain the learning process; both result in poor 3D pose predictions. Blue, green, and orange, respectively, encode the right side, middle, and left side of the human body.

keypoints to 3D by means of another trained model. A geometrically consistent 2D→3D lifting model must respect rotation-equivariance, *i.e.* as the input 2D keypoints rotate in-plane, the output 3D pose must rotate accordingly about the optical axis. Lifting models, however, typically do not exhibit this property, since it is insufficiently represented in the data they were trained on and their design does not account for it. We conjecture that incorporating the inductive bias of in-plane rotation equivariance into a lifting model without constraining the model parameter space should lead to a simpler learning process compared to one where equivariance is incorporated by design.

Therefore, we employ the common human pose estimation datasets Human3.6M [9] and MPII-INF-3DHP [14], as well as SportsCap [3], and investigate the *role of rotation equivariance* for the task of monocular 2D→3D lifting in the human pose estimation pipeline.

The scope of our work and the assumptions we make are thus as follows: **(i)** the input is a single 2D image, *i.e.* a single frame; **(ii)** the 2D keypoints are detected by a common off-the-shelf keypoint detector, *i.e.* equivariance is only investigated in lifting models; **(iii)** no additional features are provided in the input to the lifting model, besides 2D keypoints.

Our contributions are that we quantitatively and qualitatively demonstrate that for monocular 3D HPE,

- Typical lifting models are geometrically inconsistent, and they fail on rotated out-of-distribution poses
- Rotation equivariance as an inductive bias improves the performance for human poses akin to rotations in the image plane (see Figure 1)
- The correct rotation equivariance is efficiently and straightforwardly learned by augmentation, outperforming state-of-the-art methods that are equivariant by design.

2 Background

2.1 Human Pose Estimation

Monocular 3D human pose estimation is a challenging but vast field of research. Methods can be split into two categories: two-stage and end-to-end approaches.

Two-Stage Approaches Two-stage approaches decompose monocular 3D human pose estimation into two stages: 2D keypoint detection and 3D pose lifting. This allows the lifting module to focus completely on geometric reasoning.

A well-established baseline in this category is the work by Martinez *et al.* [13], which uses a lightweight fully connected network to regress 3D joint coordinates from 2D inputs. Despite its simplicity, this method achieves strong performance on Human3.6M [9] and clearly demonstrates that accurate 3D pose estimation is feasible given reliable 2D keypoints. Due to its effectiveness and minimal architectural assumptions, it remains a standard baseline for evaluating lifting-based methods, including in our work.

Subsequent research extends this paradigm by incorporating additional constraints and refinement strategies. Li *et al.* [11] propose a cascaded lifting framework with iterative refinement and data evolution to improve robustness to noisy 2D detections. Xu *et al.* [20] integrate kinematic priors directly into the lifting network, enforcing physically plausible joint relationships to reduce depth ambiguity and implausible poses. Extending lifting methods to more challenging viewpoints, Wang *et al.* [18] augment 2D keypoints with scene geometry cues, addressing severe occlusions and missing joints common in egocentric settings.

More recently, transformer-based architectures have been adopted to enhance lifting performance by modelling global spatial and temporal dependencies. PoseFormer [21] achieves improved robustness to occlusion and temporal inconsistency compared to convolutional temporal models.

End-To-End Approaches End-to-end methods aim to predict 3D human pose directly from RGB images, eliminating the explicit 2D lifting stage.

Wang *et al.* [19] introduce a unified framework that jointly performs detection and 3D pose estimation while modelling uncertainty through distribution-aware representations, enabling robust multi-person inference in crowded scenes. Earlier work from Moon *et al.* [15] incorporates camera distance estimation into a top-down pipeline to alleviate scale and depth ambiguities inherent in monocular images. Complementary to fully supervised end-to-end approaches, Wandt and Rosenhahn [17] propose RepNet, a weakly supervised adversarial reprojection framework that learns image-to-3D pose mappings using only 2D keypoint supervision.

For further reading and comprehensive overviews, we refer to these two survey papers [10, 7].

2.2 Rotation Equivariance

Rotations in n D are the actions of the special orthogonal group $\text{SO}(n)$, and can be represented with $n \times n$ matrices R such that $R^\top R = RR^\top = \mathbf{I}_n$, with \mathbf{I}_n being the identity matrix, and $\det R = 1$.

A function $f : \mathcal{X} \rightarrow \mathcal{Y}$ is said to be $\text{SO}(n)$ -equivariant, *i.e.* equivariant under n D rotations, if for every $R \in \text{SO}(n)$, in the function output space, \mathcal{Y} , there exists the transformation representation, $\rho(R)$, such that

$$\rho(R)f(X) = f(Rx) \quad \text{for all } R \in \text{SO}(n), X \in \mathcal{X} \subseteq \mathbb{R}^n. \quad (1)$$

If the transformation representation in the output space is identity, *i.e.* if for every $R \in \text{SO}(n)$, $\rho(R) = \mathbf{I}_n$, we call a function $f : \mathcal{X} \rightarrow \mathcal{Y}$ $\text{SO}(n)$ -invariant:

$$f(X) = f(Rx) \quad \text{for all } R \in \text{SO}(n), x \in \mathcal{X} \subseteq \mathbb{R}^n. \quad (2)$$

Rotation equivariance is a powerful inductive bias, and when incorporated appropriately, leads to improved and robust performance, *e.g.* in point-cloud classification [5], trajectory prediction [1], molecular properties prediction [2], and energy and force prediction for materials science applications [12].

In this work, we focus specifically on equivariance under 2D rotations, *i.e.* $\text{SO}(2)$ actions, as well as their embedding into $\text{SO}(3)$, in the context of 2D→3D lifting for monocular 3D HPE. This is unlike the DECA method [6], which is an end-to-end HPE method working on depth images, equivariant to camera viewpoint changes (*i.e.* 3D rotations of the camera around the human).

In addition, the work by Howell *et al.* [8] examines the theoretical basis for incorporating rotation equivariance constraints when learning 3D representations from 2D images. Namely, it shows that only restricted symmetry actions can be consistently defined between 2D input images and 3D outputs. While we do not build our work on this framework directly, our observations made in Section 4 are consistent with their analysis.

3 Geometrically Consistent Lifting Model

We call a lifting model, $f(X) : \mathbb{R}^{N \times 2} \rightarrow \mathbb{R}^{N \times 3}$, *geometrically consistent* if the following equivariance property holds for any $X \in \mathbb{R}^{N \times 2}$ and an in-plane rotation, $R_\theta \in \text{SO}(2)$, about the angle $\theta \in [0, 2\pi)$:

$$f(X R_\theta^\top) = f(X) \begin{bmatrix} R_\theta^\top & 0 \\ 0 & 1 \end{bmatrix}, \quad (3)$$

which means that any (global) in-plane rotation of the input 2D keypoints corresponds to a rotation about the optical axis of the output 3D point set (see Figure 2), leaving the depth-coordinate invariant.

Enforcing exact equivariance given by Eq. (3) may be too restrictive since the true 2D→3D mapping is often only approximately rotation-equivariant in

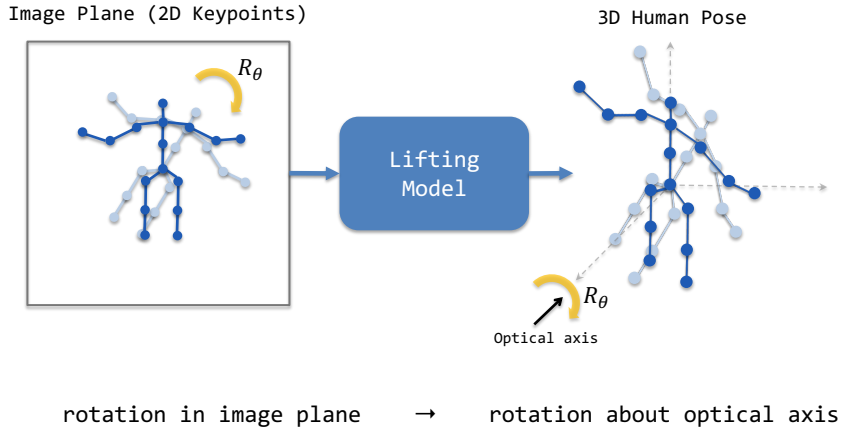


Fig. 2. Geometric consistency in the lifting model: rotations in the image plane correspond to the rotations about the optical axis in the camera coordinate system.

practice. The exact equivariance can thus prevent the model from producing an optimal prediction.

In the following section, we investigate how geometrically consistent common 2D→3D lifting models [13,21] are and how useful and limiting the constraint in Eq. (3) becomes in practice by employing the following types of models:

- **Fully equivariant**: Models that satisfy Eq. (3) exactly by design
- **Hybrid**: Models that only produce rotation-equivariant xy -coordinates by design, with a non-invariant output depth (**hybrid**) and trained to produce approximately invariant depth (**hybrid + aug**)
- **Vanilla**: Models that are non-equivariant (**vanilla**) and trained to approximately satisfy Eq. (3) by augmentation (**vanilla + aug**).

4 Experiments and Results

4.1 Models

In this section, we outline the models we build according to the types described in Section 3. We strive to conduct a fair comparison and therefore construct the models with a similar number of parameters ($\sim 3.7 - 4.4M$) determined by, when applicable, a matching number of layers and feature dimensions. Our choice of models is motivated by their relevance to the scope of our work (see Section 1), reported performance on related tasks, and reproducibility.

Fully equivariant We utilise VN-Transformer [1], a transformer architecture based on the vector neurons framework [5] for rotation-equivariant point cloud processing. In addition, we employ GotenNet [2], a state-of-the-art model for

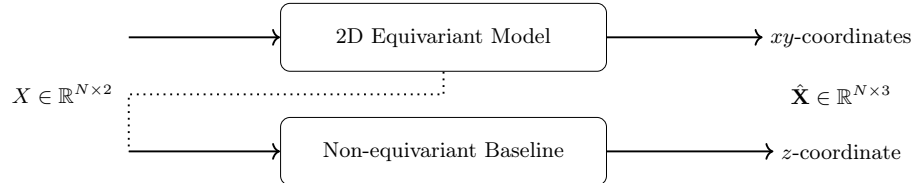


Fig. 3. Hybrid model architecture outline: the xy -outputs are rotation-equivariant, whereas the z -coordinate prediction is non-equivariant. In the default setting (no dotted line), the input is fed into both models in parallel; for the ablation study (with the dotted line), the input to the non-equivariant baseline is the output of the first equivariant layer of the 2D equivariant model.

rotation-equivariant molecular analysis, reconciling the expensive high-order equivariant interactions of concurrent methods with scalar-based approaches. We use open-source implementations³. In order to use them, we need to ensure that the input joints (2D) are in the same dimension as the output (3D). While we can use a constant value as the third coordinate for all input points for VN-Transformer (*e.g.* 1), this does not work for GotenNet due to the joint-wise differences used in the model, which leads to the third coordinate in the output always being zero. Thus, for both models, we append every $N \times 2$ input with a vector of size N sampled randomly only once when the model is instantiated.

Vanilla We use the simple ResNet-based baseline by Martinez *et al.* [13], as well as a transformer-based baseline, PoseFormer, by Zheng *et al.* [21]. These vanilla models do not consider rotation equivariance in their 3D human pose estimates, thus failing when encountering a rotated out-of-distribution pose, as seen in the example in Fig. 1. The architecture from Martinez *et al.* [13] consists of two sequential blocks of ResNet, taking the flattened 2D pose as input vector, and outputs the corresponding 3D pose vector. The PoseFormer [21] models the spatial and temporal correlation between human joints via the transformer architecture. Originally, PoseFormer is designed to take in a sequence of 2D poses as input. To maintain fair comparison, we modify the architecture of PoseFormer to work with single-frame inputs, by reducing the length of input sequence to 1 and decreasing the depth of the temporal transformer module to 2, resulting in a comparable number of learnable parameters.

Hybrid In order to analyse the potential limitation of the expensiveness of fully equivariant models mentioned in Section 3, we combine an equivariant model, VN-Transformer or GotenNet, used for xy -prediction only, with the ResNet baseline [13] predicting the depth coordinate, as shown in Figure 3. Given the VN-Transformer implementation, we straightforwardly instantiate it for 2D, whereas

³ <https://github.com/lucidrains/VN-transformer> and <https://github.com/lucidrains/gotennet-pytorch>, respectively.

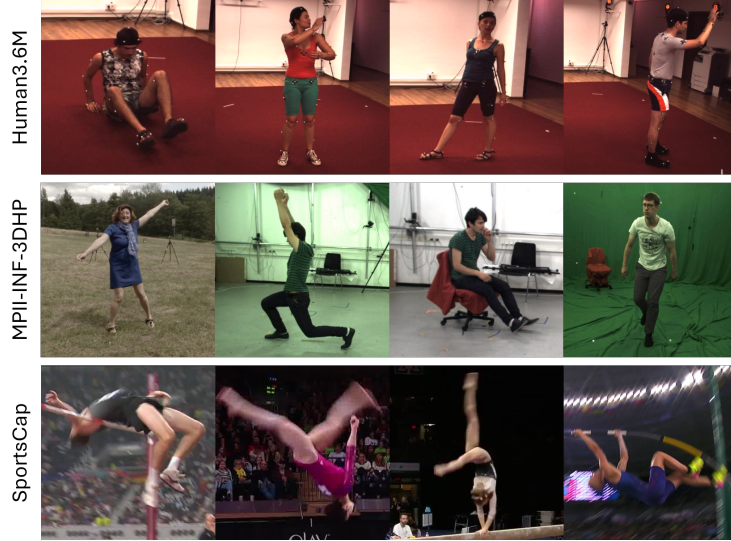


Fig. 4. Samples from the datasets used in our experiments. SportsCap contains poses with realistic full-body rotations that do not exist in the Human3.6M and the MPII-INF-3DHP datasets.

the GotenNet implementation is optimised for 3D, and we run it as-is by initialising the third coordinate to 0 and extracting the first two coordinates for each joint in the output pose. In both cases, we reduce the number of parameters of the equivariant models to keep the same non-equivariant baseline ResNet, so that the total number of parameters falls within the range of the other models in comparison.

4.2 Datasets

We first train the model on the Human3.6M dataset [9], which contains diverse motion capture data in a laboratory setup. Following the standard training protocol [13,21], we use the first five subjects (S1, S5, S6, S7, S8) for training and the remaining two (S9, S11) for testing. To examine the generalisation of the models, we additionally evaluate them on the test set of the MPII-INF-3DHP dataset [14] without any fine-tuning. Besides the two common datasets, Human3.6M and MPII-INF-3DHP, that mostly contain simple standing and walking poses, we propose an additional evaluation on the more challenging SportsCap dataset [3] (without 3D ground truth) containing complex gymnastics poses with realistic full-body rotations that do not exist in the Human3.6M and MPII-INF-3DHP datasets (see Figure 4).

Method	Type	Human3.6M		MPII-INF-3DHP	
		Original	Rotated	Original	Rotated
ResNet [13]	Vanilla	62.9 ± 0.2	209.6 ± 1.4	144.0 ± 0.7	225.8 ± 2.9
ResNet+aug	Vanilla	<u>64.2 ± 0.1</u>	64.3 ± 0.1	152.3 ± 1.1	152.6 ± 1.4
PoseFormer [21]	Vanilla	65.9 ± 0.1	232.4 ± 5.2	139.9 ± 0.7	247.5 ± 5.7
PoseFormer+aug	Vanilla	65.1 ± 0.1	<u>65.0 ± 0.2</u>	145.7 ± 4.1	146.2 ± 1.8
VNTransformer [1]	Fully equi.	76.4 ± 1.2	76.4 ± 1.2	171.2 ± 2.0	171.2 ± 2.0
VNTransformer+aug	Fully equi.	76.8 ± 1.0	76.8 ± 1.0	174.5 ± 9.2	174.5 ± 9.2
GotenNet [2]	Fully equi.	76.7 ± 1.3	76.7 ± 1.3	169.4 ± 5.7	169.4 ± 5.7
GotenNet+aug	Fully equi.	76.8 ± 1.3	76.8 ± 1.3	171.9 ± 3.0	171.9 ± 3.0
VNTransformer	Hybrid	<u>64.2 ± 0.1</u>	176.8 ± 1.0	153.2 ± 2.1	212.0 ± 2.2
VNTransformer+aug	Hybrid	66.0 ± 0.4	66.0 ± 0.3	160.1 ± 7.4	160.2 ± 6.9
GotenNet	Hybrid	64.3 ± 0.3	177.5 ± 0.8	<u>143.7 ± 4.3</u>	206.0 ± 3.1
GotenNet+aug	Hybrid	65.8 ± 0.2	65.9 ± 0.3	151.1 ± 0.6	<u>150.8 ± 1.2</u>

Table 1. Quantitative results with evaluation *Protocol 1* on the *Original* and *Rotated* test sets of Human3.6M and MPII-INF-3DHP. The best results are highlighted in **bold**, and the second-best results are underlined.

Metrics We use the mean per-joint position error (MPJPE) as the main evaluation metric for comparisons. The MPJPE measures the average L2 distance between the estimated 3D human poses $\hat{\mathbf{X}} \in \mathbb{R}^{N \times 3}$ and ground truth $\mathbf{X} \in \mathbb{R}^{N \times 3}$ in millimetre (mm), computed as:

$$\text{MPJPE}(\mathbf{X}, \hat{\mathbf{X}}) = \frac{1}{N} \sum_{n=1}^N \|\mathbf{X} - \hat{\mathbf{X}}\|_2. \quad (4)$$

In Table 1, we refer the MPJPE metric as *Protocol 1*. We also report the Procrustes-aligned mean per-joint position error (PA-MPJPE), commonly known as *Protocol 2*, in Table 2. The PA-MPJPE eliminates global rotation, translation, and scaling errors, focusing more on the local joint pose error between the estimations and ground truth.

4.3 Implementation Details

Training details We use PyTorch [16] in our experiments. The inputs to the models are the 2D poses collected from an off-the-shelf estimator HRNet [4]. The input 2D poses are standardised to a zero mean and a standard deviation of one. The ground-truth 3D poses are in camera coordinates and root-aligned at the origin. All models are trained to minimise the mean squared error (MSE) between the ground truth and estimated human poses, for a total of 100 epochs on the training set of the Human3.6M dataset, with a batch size of 1024 (reduced to 512 for GotenNet due to computational constraints), Adam optimiser, an initial learning rate of 10^{-3} , and the ExponentialLR scheduler with $\gamma = 0.96$.

Method	Type	Human3.6M		MPII-INF-3DHP	
		<i>Original</i>	<i>Rotated</i>	<i>Original</i>	<i>Rotated</i>
ResNet [13]	Vanilla	44.5 ± 0.1	109.1 ± 0.8	<u>99.3 ± 0.4</u>	134.6 ± 1.0
ResNet+aug	Vanilla	46.2 ± 0.1	46.2 ± 0.1	102.6 ± 2.0	<u>102.6 ± 1.4</u>
PoseFormer [21]	Vanilla	47.9 ± 0.1	127.0 ± 1.6	97.4 ± 1.0	141.4 ± 1.0
PoseFormer+aug	Vanilla	46.6 ± 0.1	<u>46.5 ± 0.2</u>	101.3 ± 2.9	101.9 ± 1.9
VNTransformer [1]	Fully equi.	56.2 ± 0.8	56.2 ± 0.8	124.0 ± 2.8	124.0 ± 2.8
VNTransformer+aug	Fully equi.	56.3 ± 0.6	56.3 ± 0.6	126.5 ± 5.7	126.5 ± 5.7
GotenNet [2]	Fully equi.	55.5 ± 0.7	55.5 ± 0.7	125.5 ± 5.3	125.5 ± 5.3
GotenNet+aug	Fully equi.	55.8 ± 0.6	55.8 ± 0.6	126.5 ± 2.3	126.5 ± 2.3
VNTransformer	Hybrid	<u>45.6 ± 0.1</u>	101.2 ± 0.7	106.2 ± 0.8	134.4 ± 1.5
VNTransformer+aug	Hybrid	46.8 ± 0.2	46.8 ± 0.2	110.6 ± 4.5	110.1 ± 3.6
GotenNet	Hybrid	<u>45.6 ± 0.1</u>	102.2 ± 1.0	101.3 ± 3.5	130.1 ± 1.0
GotenNet+aug	Hybrid	46.9 ± 0.1	47.0 ± 0.1	105.2 ± 1.0	104.1 ± 1.1

Table 2. Quantitative results with evaluation *Protocol 2* on the test sets of Human3.6M and MPII-INF-3DHP. The best results are highlighted in **bold**, and the second-best results are underlined.

Data augmentation When specified `+aug`, we perform data augmentation by randomly transforming the input $X \in \mathbb{R}^{N \times 2}$ and the xy -coordinates of the corresponding target pose $\mathbf{X} \in \mathbb{R}^{N \times 3}$ with the same rotation R_θ . The rotation angle θ is sampled from a uniform distribution during training. To evaluate the equivariance property, we also apply random rotations to the test data in the same way, when specified *Rotated*.

Computational resources All experiments are conducted on the NVIDIA A100 devices with 40GB of memory. To demonstrate the reproducibility, each model is evaluated on three different random seeds. The mean error and standard deviation across three runs are reported for the quantitative results. The training and inference times are presented in Table 3.

4.4 Results and Discussion

The results presented in Tables 1 and 2 consistently demonstrate that the vanilla lifting models do not learn the equivariance property from the data (see the performance on the *Original* vs. *Rotated*). However, we straightforwardly solve this by augmentation, resulting in vanilla+aug models outperforming both fully equivariant and hybrid+aug models, across all the *Rotated* datasets. Notably, the performance of the `+aug` models, in most cases, is slightly reduced on the *Original* datasets, since they do not contain poses resembling full-body rotations.

Furthermore, the domain generalisation of the vanilla models (see *Original* MPII-INF-3DHP results) and vanilla+aug models (see *Rotated* MPII-INF-3DHP results) is better than that of other models, suggesting that the augmentation does not incur overfitting to a specific dataset.

Method	Type	Training time (1 epoch)	Inference time (1 sample)
ResNet [13]	Vanilla	11 s	0.39 ms
ResNet+aug	Vanilla	<u>34 s</u>	0.39 ms
PoseFormer [21]	Vanilla	26 s	<u>2.23 ms</u>
PoseFormer+aug	Vanilla	48 s	<u>2.23 ms</u>
VNTransformer [1]	Fully equi.	5 m 18 s	4.28 ms
VNTransformer+aug	Fully equi.	5 m 18 s	4.28 ms
GotenNet* [2]	Fully equi.	11 m 5 s	14.38 ms
GotenNet+aug*	Fully equi.	11 m 7 s	14.38 ms
VNTransformer	Hybrid	46 s	4.68 ms
VNTransformer+aug	Hybrid	47 s	4.68 ms
GotenNet	Hybrid	3 m 41 s	14.68 ms
GotenNet+aug	Hybrid	3 m 43 s	14.68 ms

Table 3. Training and inference time comparison. The most accurate models (vanilla+aug) have both the shortest training and inference times. *The fully equivariant GotenNet uses batch size 512 due to computational constraints. The best results are highlighted in **bold**, and the second-best results are underlined.

Overall, the relation between the performance of the different model types on the *Rotated* datasets can be written as

$$\text{vanilla+aug} > \text{hybrid+aug} > \text{fully equivariant} > \text{hybrid} > \text{vanilla}$$

confirming our intuition that strictly imposing the equivariance constraint Eq. (1) on a lifting model harms the task performance while guaranteeing robustness to rotations by design. Coherently, hybrid+aug models are closer in performance to that of vanilla+aug, indicating that relaxing the equivariance constraint (the rotation-invariance of the depth prediction in this case) is a step in the right direction.

These observations are consistently supported by the qualitative examples presented in Figures 5 and 6, where vanilla+aug models demonstrate more accurate 3D pose estimations. More qualitative results are shown in Figures 7 and 8.

Remarkably, the best performing models (vanilla+aug) are also among the fastest to train and have the fastest inference, as presented in Table 3. While the augmentation adds to the training time, in total it constitutes only an insignificant fraction of the training time required by fully equivariant models.

All in all, the baseline ResNet [13] endowed with equivariance learned by augmentation clearly exhibits a favourable performance/training/inference trade-off, followed closely by PoseFormer+aug.

Hybrid model ablation We also conduct an ablation study for the hybrid models by using the first layer equivariant model features for the depth prediction (see Figure 3). The results presented in Table 4 suggest that no improvement is gained compared to the original hybrid models, despite the parameter count increase caused by the growth of the dimensionality in the input to the non-equivariant baseline for depth-prediction.

Method	Type	Human3.6M		MPII-INF-3DHP	
		<i>Original</i>	<i>Rotated</i>	<i>Original</i>	<i>Rotated</i>
VNTransformer	Hybrid	64.2 \pm 0.1	176.8 \pm 1.0	153.2 \pm 2.1	212.0 \pm 2.2
VNTransformer	Hybrid 2	64.2 \pm 0.4	170.2 \pm 1.1	150.7 \pm 1.4	214.6 \pm 3.0
VNTransformer+aug	Hybrid	66.0 \pm 0.4	66.0 \pm 0.3	160.1 \pm 7.4	160.2 \pm 6.9
VNTransformer+aug	Hybrid 2	66.1 \pm 0.7	66.1 \pm 0.6	161.3 \pm 3.3	162.5 \pm 2.2
GotenNet	Hybrid	64.3 \pm 0.3	177.5 \pm 0.8	143.7 \pm 4.3	206.0 \pm 3.1
GotenNet	Hybrid 2	64.2 \pm 0.2	166.2 \pm 0.5	143.8 \pm 2.3	203.2 \pm 2.1
GotenNet+aug	Hybrid	65.8 \pm 0.2	65.9 \pm 0.3	151.1 \pm 0.6	150.8 \pm 1.2
GotenNet+aug	Hybrid 2	66.0 \pm 0.3	66.0 \pm 0.3	149.0 \pm 1.6	147.4 \pm 1.9

Table 4. Hybrid models ablation: Quantitative results with evaluation *Protocol 1* on the *Original* and *Rotated* test sets of Human3.6M and MPII-INF-3DHP. Hybrid 2 are models using the equivariant model first layer features (see Figure 3), resulting in the change of architecture of the non-equivariant baseline and the corresponding increase of the parameter count (6.5M vs. 4.4M for VN-Transformer Hybrid, and 5.3M vs. 4.3M for GotenNet Hybrid).

5 Conclusions

In this work, we investigated the role of rotation equivariance in the 2D \rightarrow 3D lifting stage of the monocular human pose estimation pipeline. We found that typical lifting models do not learn this equivariance property, failing on the poses resembling full-body rotations. We also examined different ways of endowing the model with rotation equivariance, and concluded that it can be efficiently and straightforwardly learned by augmentation, outperforming state-of-the-art equivariant-by-design methods.

Limitations The scope of our work, as outlined in Section 1, *per se*, constitutes the main limitations of our work. The selection of the models designed specifically for human pose estimation was conducted using our work scope as the main criterion, as well as the reported performance of the models and their official implementation availability (which affects the reproducibility of the published results). The selection of the equivariant models was done considering their reported state-of-the-art performance on point set/point cloud tasks.

Future work The methodology of this work can be applied to analysing temporal and probabilistic lifting models, as well as lifting models incorporating more features beyond 2D keypoints, and end-to-end methods. The application scope can also be extended beyond human pose estimation and rotation symmetries.

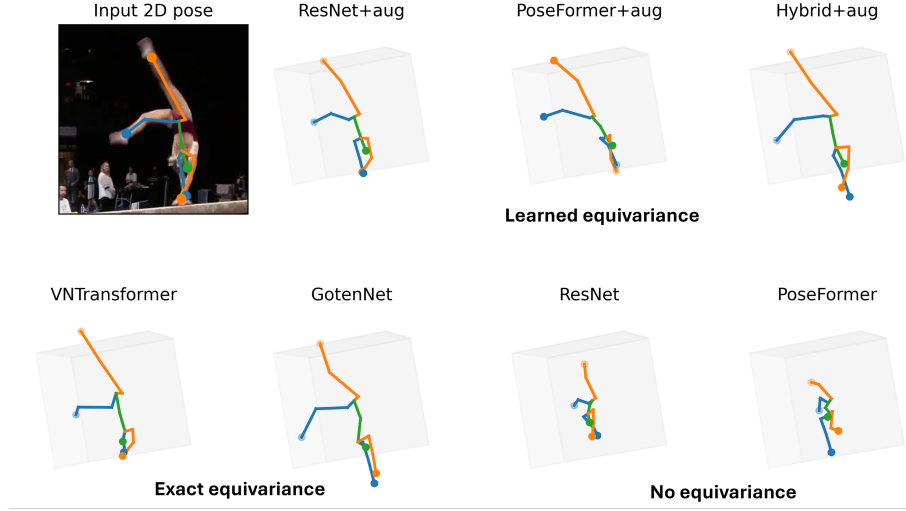


Fig. 5. Representative example of the performance of different models on a SportsCap sample: Learned equivariance in ResNet+aug and PoseFormer+aug (both vanilla+aug), as well as GotenNet hybrid+aug, produces more accurate 3D poses than exact equivariance (fully equivariant), or no equivariance (vanilla). All 3D estimation results are captured from the same viewing angle.

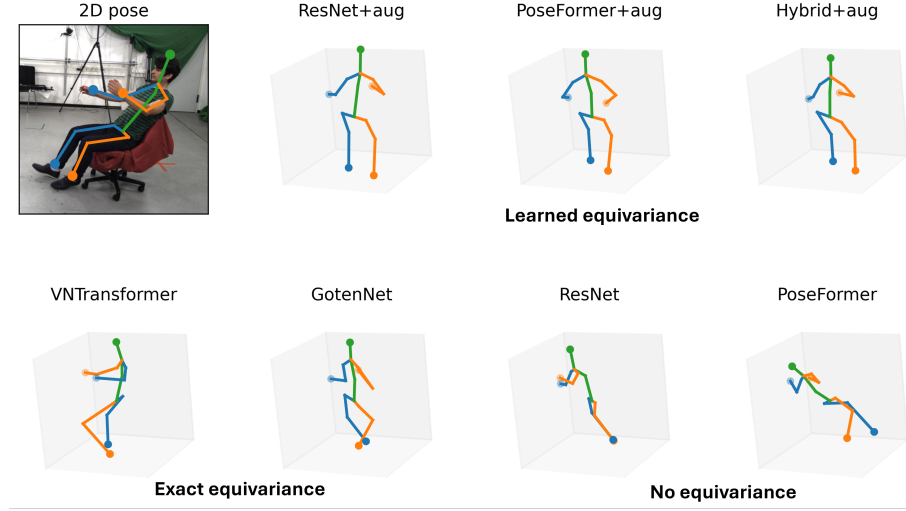


Fig. 6. An example of the performance of different models on a MPII-INF-3DHP sample that resembles a slight in-plane rotation: Learned equivariance in ResNet+aug and PoseFormer+aug (both vanilla+aug), as well as GotenNet hybrid+aug, produces more accurate 3D poses than exact equivariance (fully equivariant), or no equivariance (vanilla). All 3D estimation results are captured from the same viewing angle.

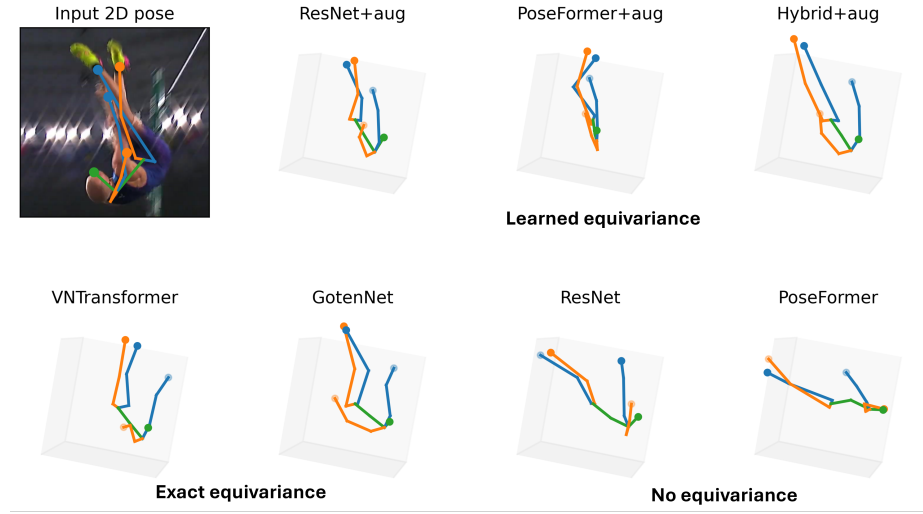


Fig. 7. An example from SportsCap. The 3D poses are observed from rear view with respect to the camera.

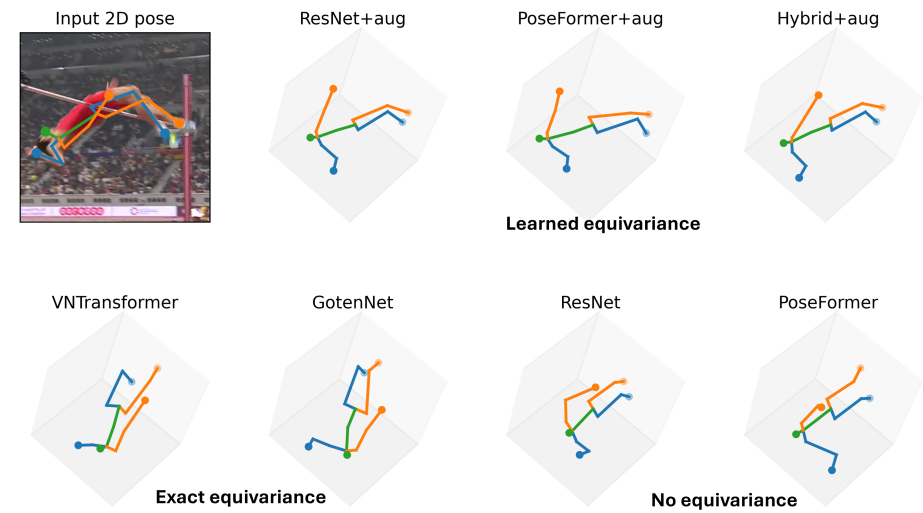


Fig. 8. An example from SportsCap. The 3D poses are observed from top view.

Acknowledgments

This work was supported by the Wallenberg AI, Autonomous Systems and Software Program (WASP), by the Swedish Research Council (VR) through a grant for the projects Uncertainty-Aware Transformers for Regression Tasks in Computer Vision (2022-04266) and Dorsal Stream Robot Vision (2022-04206), and the strategic research environment ELLIIT. The computations were enabled by resources provided by the National Academic Infrastructure for Supercomputing in Sweden (NAIIS), partially funded by the Swedish Research Council through grant agreement no. 2022-06725.

References

1. Assaad, S., Downey, C., Al-Rfou, R., Nayakanti, N., Sapp, B.: Vn-transformer: Rotation-equivariant attention for vector neurons. *TMLR* (2023)
2. Aykent, S., Xia, T.: GotenNet: Rethinking Efficient 3D Equivariant Graph Neural Networks. In: *ICLR* (2025)
3. Chen, X., Pang, A., Yang, W., Ma, Y., Xu, L., Yu, J.: Sportscap: Monocular 3d human motion capture and fine-grained understanding in challenging sports videos. *IJCV* (Aug 2021)
4. Cheng, B., Xiao, B., Wang, J., Shi, H., Huang, T.S., Zhang, L.: Higherhrnet: Scale-aware representation learning for bottom-up human pose estimation. In: *CVPR* (2020)
5. Deng, C., Litany, O., Duan, Y., Poulenard, A., Tagliasacchi, A., Guibas, L.J.: Vector neurons: A general framework for $SO(3)$ -equivariant networks. In: *CVPR* (2021)
6. Garau, N., Bisagno, N., Bródka, P., Conci, N.: DECA: Deep viewpoint-Equivariant human pose estimation using Capsule Autoencoders. In: *ICCV* (2021)
7. Guo, Y., Gao, T., Dong, A., Jiang, X., Zhu, Z., Wang, F.: A survey of the state of the art in monocular 3d human pose estimation: Methods, benchmarks, and challenges. *Sensors* (Basel, Switzerland) **25**(8), 2409 (2025)
8. Howell, O., Klee, D., Biza, O., Zhao, L., Walters, R.: Equivariant Single View Pose Prediction via Induced and Restriction Representations. *NeurIPS* (2023)
9. Ionescu, C., Papava, D., Olaru, V., Sminchisescu, C.: Human3.6m: Large scale datasets and predictive methods for 3d human sensing in natural environments. *PAMI* **36**(7), 1325–1339 (2014)
10. Ji, X., Fang, Q., Dong, J., Shuai, Q., Jiang, W., Zhou, X.: A survey on monocular 3d human pose estimation. *Virtual Reality & Intelligent Hardware* **2**(6), 471–500 (2020)
11. Li, S., Ke, L., Pratama, K., Tai, Y.W., Tang, C.K., Cheng, K.T.: Cascaded deep monocular 3d human pose estimation with evolutionary training data. In: *CVPR* (2020)
12. Liao, Y.L., Wood, B., Das, A., Smidt, T.: EquiformerV2: Improved Equivariant Transformer for Scaling to Higher-Degree Representations. *ICLR* (2024)
13. Martinez, J., Hossain, R., Romero, J., Little, J.J.: A simple yet effective baseline for 3d human pose estimation. In: *ICCV* (2017)
14. Mehta, D., Rhodin, H., Casas, D., Fua, P., Sotnychenko, O., Xu, W., Theobalt, C.: Monocular 3d human pose estimation in the wild using improved cnn supervision. In: *3DV* (2017), http://gvv.mpi-inf.mpg.de/3dhp_dataset

15. Moon, G., Chang, J.Y., Lee, K.M.: Camera distance-aware top-down approach for 3d multi-person pose estimation from a single rgb image. In: ICCV (2019)
16. Paszke, A., Gross, S., Massa, F., Lerer, A., Bradbury, J., Chanan, G., Killeen, T., Lin, Z., Gimelshein, N., Antiga, L., et al.: Pytorch: An imperative style, high-performance deep learning library. NeurIPS (2019)
17. Wandt, B., Rosenhahn, B.: Repnet: Weakly supervised training of an adversarial reprojection network for 3d human pose estimation. In: CVPR (2019)
18. Wang, J., Luvizon, D., Xu, W., Liu, L., Sarkar, K., Theobalt, C.: Scene-aware egocentric 3d human pose estimation. In: CVPR (2023)
19. Wang, Z., Nie, X., Qu, X., Chen, Y., Liu, S.: Distribution-aware single-stage models for multi-person 3d pose estimation. In: CVPR (2022)
20. Xu, J., Yu, Z., Ni, B., Yang, J., Yang, X., Zhang, W.: Deep kinematics analysis for monocular 3d human pose estimation. In: CVPR (2020)
21. Zheng, C., Zhu, S., Mendieta, M., Yang, T., Chen, C., Ding, Z.: 3d human pose estimation with spatial and temporal transformers. ICCV (2021)